

Broad-band Time Domain Modeling of Sonar Clutter in Range Dependent Waveguides

K. D. LePage
Naval Research Lab.
4445 Overlook Ave., SW
Washington, DC 20375

P. Neumann
Planning Systems Inc.
290 Village Park Drive
Lebanon, OH 45036

C. W. Holland
Pennsylvania State Univ., Applied Research Lab.
PO Box 30
State College, PA 16804

Abstract—A broadband time domain reverberation and clutter model has been developed to aid in the development of a better understanding of the environmental and system characteristics which drive sonar clutter in inhomogeneous waveguides. The theoretical background of the model is presented and its ability to model both diffuse background reverberation levels and clutter characteristics for a site on the Malta Plateau south of Sicily are evaluated.

I. INTRODUCTION

Sonar clutter in littoral environments increases the probability of false alarm for a given probability of detection. This is because clutter adds to the length of the tails of the reverberation envelope probability distribution function (*pdf*), moving the statistics away from the Rayleigh canonical form. Clutter can be caused by target-like features, either natural or man-made, or by non-Gaussian distributions of the scatterers. Typically, high bandwidth and/or highly directive systems have more problems with clutter, because as the size of the scattering patch is reduced, the *pdf* of the generally non-Gaussian scatterer distributions becomes resolved by the system. Recent work [1] has demonstrated that for single path saturated propagation to a collection of exponentially sized scatterers, the scattering envelope has the analytic form of the K distribution, in the physical optics limit. The K distribution shape parameter, which controls the degree of non-Rayleighness of the scattering envelope, was shown in turn to be directly proportional to the number of scatterers within the sonar

footprint. For scatterer numbers greater than approximately 40, the scattered envelope was shown to revert to Rayleigh.

For reverberation in inhomogeneous, range dependent shallow water waveguides, it becomes necessary to generalize the results of Abraham and Lyons to obtain predictions of interest for notional sonar systems. In range independent waveguides the propagation physics along with the system's directivity and bandwidth control the number of scatterers that contribute to the reverberation envelope statistics. For example, for rough surfaces, the shallow angle paths which persist the longest due to low attenuation, and travel the fastest due to the higher group speeds, generally also generate the least amount of scattering locally from a given roughness distribution. Conversely, the heavily attenuated steeper, slower paths generate relatively more scattering locally for a given level of incident intensity. This means that there is a trade-off of the different paths as a function of range, with the steeper paths being dominant at short range and the shallower paths becoming more important at long range [2]. The dispersion of the waveguide, which leads to time spread, together with the bandwidth determine the degree to which the various multipath contributions to the reverberation are independent. The number of range-wise scatterers contributing to reverberation is controlled by the bottom critical angle, the vertical directivity of the source, the scattering angle dependence of the scattering kernel, the loss vs. angle relation of the bottom interaction loss, and the bandwidth, while it is the horizontal beamwidth alone that controls the number of independent azimuthal scatterers contributing to the reverberation for the monostatic systems considered here.

Work supported by ONR Phase II STTR N00014-04-C-0399 "Advanced Physics-Based Modeling of Discrete Clutter and Diffuse Reverberation in the Littoral Environment".

Report Documentation Page				Form Approved OMB No. 0704-0188	
Public reporting burden for the collection of information is estimated to average 1 hour per response, including the time for reviewing instructions, searching existing data sources, gathering and maintaining the data needed, and completing and reviewing the collection of information. Send comments regarding this burden estimate or any other aspect of this collection of information, including suggestions for reducing this burden, to Washington Headquarters Services, Directorate for Information Operations and Reports, 1215 Jefferson Davis Highway, Suite 1204, Arlington VA 22202-4302. Respondents should be aware that notwithstanding any other provision of law, no person shall be subject to a penalty for failing to comply with a collection of information if it does not display a currently valid OMB control number.					
1. REPORT DATE 01 SEP 2006		2. REPORT TYPE N/A		3. DATES COVERED -	
4. TITLE AND SUBTITLE Broad-band Time Domain Modeling of Sonar Clutter in Range Dependent Waveguides				5a. CONTRACT NUMBER	
				5b. GRANT NUMBER	
				5c. PROGRAM ELEMENT NUMBER	
6. AUTHOR(S)				5d. PROJECT NUMBER	
				5e. TASK NUMBER	
				5f. WORK UNIT NUMBER	
7. PERFORMING ORGANIZATION NAME(S) AND ADDRESS(ES) Naval Research Lab. 4445 Overlook Ave., SW Washington, DC 20375				8. PERFORMING ORGANIZATION REPORT NUMBER	
9. SPONSORING/MONITORING AGENCY NAME(S) AND ADDRESS(ES)				10. SPONSOR/MONITOR'S ACRONYM(S)	
				11. SPONSOR/MONITOR'S REPORT NUMBER(S)	
12. DISTRIBUTION/AVAILABILITY STATEMENT Approved for public release, distribution unlimited					
13. SUPPLEMENTARY NOTES See also ADM002006. Proceedings of the MTS/IEEE OCEANS 2006 Boston Conference and Exhibition Held in Boston, Massachusetts on September 15-21, 2006, The original document contains color images.					
14. ABSTRACT					
15. SUBJECT TERMS					
16. SECURITY CLASSIFICATION OF:			17. LIMITATION OF ABSTRACT UU	18. NUMBER OF PAGES 5	19a. NAME OF RESPONSIBLE PERSON
a. REPORT unclassified	b. ABSTRACT unclassified	c. THIS PAGE unclassified			

In order to incorporate the above considerations into developing a better understanding of the environmental and system drivers of sonar clutter in inhomogeneous waveguides, a broadband time domain monostatic reverberation/clutter model has been developed based on the R-SNAP model [2]. The R-SNAP model is based on the theory of coupled normal modes and exploits the knowledge of modal group speeds and dispersion to generate approximate reverberation time series using the narrow band approximation. Until now the model has been used solely to predict the reverberation intensity of monostatic systems as a function of the environmental and system parameters, although it was also capable of predicting the backscattered levels returned from deterministic environmental discontinuities in the submarine environment. Here the model has been extended to generate reverberation time series consistent with the closed form intensity estimates, generated in a Monte-Carlo manner from realizations of the bottom scatterers. In this paper we describe the theoretical background of the model and evaluate its ability to model both diffuse background reverberation levels and clutter characteristics for a site on the Malta Plateau south of Sicily.

II. THEORY

A. Reverberation Simulation

The R-SNAP model is based on the C-SNAP coupled normal mode propagation model [3]. In C-SNAP the total field at a scatterer depth z_{scat} is given as a function of the range dependent complex modal amplitude a_n and the range dependent mode depth functions ϕ_n

$$p(r, z_{scat}) = \sum_{n=1}^N a_n(r) \phi_n(r, z_{scat}), \quad (1)$$

In R-SNAP we are instead interested in the field incident on the scattering plane at the scatterer depth. This is accomplished by decomposing the mode shape functions ϕ into up and down-propagating plane waves ϕ^\pm [4]. The field incident on the scattering plane at depth z_{scat} is then

$$p^-(r, z_{scat}) = \sum_{n=1}^N a_n(r) \phi_n^-(r, z_{scat}), \quad (2)$$

and the field backscattered from an array of objects at ranges r' with a scattering function $ss(r, \theta_n, \theta_m)$ is then given as

$$p_{rev}(r, z_r) = \sum_{n=1}^N \sum_{m=1}^N \int_{r=0}^{\infty} a_n(r') \phi_n^-(r', z_{scat}) ss(r', \theta_n, \theta_m) \phi_m^+(r', z_{scat}) a_m(r') dr'. \quad (3)$$

Equation (3) is an expression for the scattered field in the frequency domain. Since reverberation is observed in the time domain, the Fourier transform of (3) is required to perform a simulation. This Fourier transform can be well approximated in the case of relatively narrowband

excitation through the use of the narrowband approximation for coupled propagation in range dependent media [5]. For one-way propagation the narrowband approximation for range dependent waveguides is

$$p(t, r, z_r) = 2 \operatorname{Re} \left\{ \sum_{n=1}^N \frac{\sqrt{2\pi} a_n(r') \phi_n(r', z_{scat})}{\sqrt{1/\Delta\omega^2 - d_n(r)r}} \exp \left(-i\omega t - \frac{(t - s_n(r)r)^2}{2(1/\Delta\omega^2 - d_n(r)r)} \right) \right\}, \quad (4)$$

where ω is the frequency at which the solution to (1) was obtained, s_n is the first derivative of the mode n wavenumber k_n with respect to circular frequency, d_n is the corresponding second derivative, and $\Delta\omega$ is the bandwidth of the source signal in rad/s.

B. Scattering Strength Decomposition

In the work [1] on single path scattering statistics, the scattering strength of the spheres with exponentially distributed radii was

$$ss(r) = a/2, \quad (5)$$

the geometric optics limit for a rigid scatterer. For rough surface scattering, we argue that the scattering strength may be decomposed into the product of an angularly dependent term and a spatial distribution. Whereas in [1] the spatial distribution was discrete with sufficient spatial randomness to guarantee phase saturation, in rough surface scattering we are dealing with a continuous distribution. Thus our model is

$$ss(r, \theta_n, \theta_m) = \eta(r) f(\omega, \theta_n, \theta_m, \mathbf{E}), \quad (6)$$

where η is the height profile of the roughness, $\theta_{n,m}$ are the incident and scattered grazing angles associated with modes n and m , and \mathbf{E} is a vector of environmental information containing information about the water and bottom sound speeds, densities and attenuations. In this case it may be shown that under the first order perturbation approximation [6]

$$f(\omega, \theta_n, \theta_m, \mathbf{E}) = -k_{zm} \mathbf{B}_E^{-1}(k_m) \left(\frac{\partial \mathbf{B}_E(k_n)}{\partial z} - i(k_n + k_m) \mathbf{b}_E(k_n) \right) \bar{p}_E(k_n), \quad (7)$$

where \mathbf{B} is the boundary condition operator for the unperturbed boundary described by \mathbf{E} at the rough surface, \mathbf{b} is an associated rotational operator, and $\bar{p}(k_n)$ is a vector containing a unity amplitude plane wave incident on the mean scattering surface at the grazing angle associated with mode n , along with the associated reflected and

transmitted components for the unperturbed boundary described by \mathbf{E} .

An analogous description for arbitrary scattering strength angular dependence may also be utilized. As long as the correlation length scale of the scatterer distribution is smaller than half an incident wavelength, a very good approximation is

$$f(\omega, \theta_n, \theta_m, \mathbf{E}) = 10^{SS(\omega, \theta_n, \theta_m)/20}, \quad (8)$$

where $SS(\omega, \theta_n, \theta_m)$ is some parametric form of the scattering strength, derived from data for instance.

III. MALTA PLATEAU DATA

A. Reverberation Characteristics

The Malta Plateau is a shallow (70-200 m) site in the Straits of Sicily north of Malta. It is characterized by a muddy bottom lying over consolidated sediment/rock which becomes exposed in a ridge running north-south between Malta and eastern Sicily. In Fig. 1 the sediment thickness to the consolidated sediment is illustrated in color with the bathymetric contours superimposed.

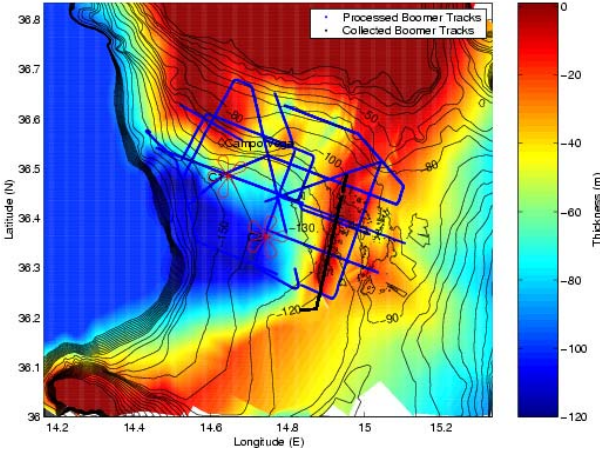


Figure 1. Sediment thickness and bathymetry on the Malta Plateau.

In Fig. 2 reverberation smoothed by a 33 ms rectangle from a 91 m SUS charge for this site is illustrated in the 100Hz-2kHz band. This data was collected during the SCARAB 98 trial conducted by SACLANTCEN (now NATO Undersea Research Centre (NURC)). Clearly evident is the dominant scattering from the region of shoaling bathymetry and thinning sediment cover associated with the Ragusa ridge. Also evident are strong scattering events from certain known wrecks to the South and East of the source and the Campo Vega oil production platform to the NNW (approximate locations are indicated by the superimposed black symbols).

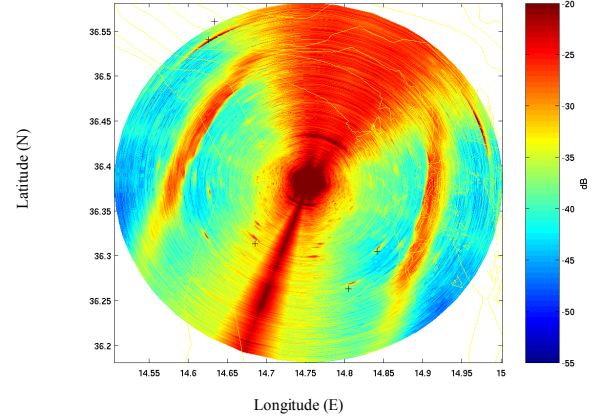


Figure 2. Reverberation data collected on the Malta Plateau.

We are interested in the characteristics of clutter in shallow water reverberation datasets such as illustrated in Fig. 2. Clearly there are at least two types of clutter in this data set: diffuse clutter characterized by increased reverberation from the exposed ridge, and discrete clutter events associated with anthropogenic sources such as shipwrecks and oil productions facilities. In Fig. 3 we show the spectrogram of the return seen on the bearing of 116 true from Fig. 2. Here one can observe the broadband nature of both the discrete clutter event seen at 15 s and the extended return from the Ragusa ridge from 19 to 24 s. One also observes many other smaller clutter events, most energetic between 1 and 2 kHz. Superimposed on these features is the time-frequency structure of coherent round-trip propagation to the scatterers in the waveguide, characterized by a clearly visible striation pattern.

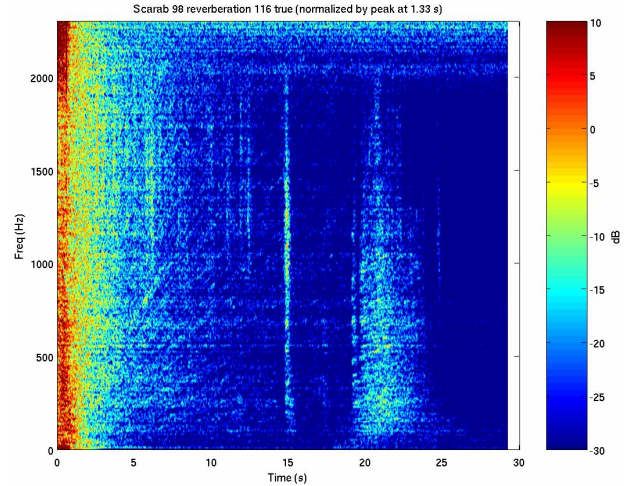


Figure 3. Time-frequency spectrogram of SUS reverb looking towards shipwreck and Ragusa ridge.

B. Environmental Description

A detailed geoacoustic and scattering description of the environment between Sicily and Malta has been prepared based on measurements of propagation, scattering strength and reverberation. The results are shown in Table 1. Notice that both the sediment attenuation and the scattering strength grow linearly with frequency. Use of the values in Table 1 give good agreement with the background levels of reverberation on the sediments of the Malta Plateau, away from the Ragusa ridge [7].

TABLE I
BACKGROUND ENVIRONMENTAL PROPERTIES FOR MALTA PLATEAU

Property	Value
Sediment Sound Speed Ratio	1.05
Sediment Density	1.80 gm/cm ³
Sediment Attenuation (dB/λ)	0.70 f (f in kHz)
Sediment Scattering Strength (Lommel-Seeliger)	-47+14.8 f (f in kHz) dB
Ridge Scattering Strength (Lommel-Seeliger)	-15 dB

IV. SIMULATION RESULTS

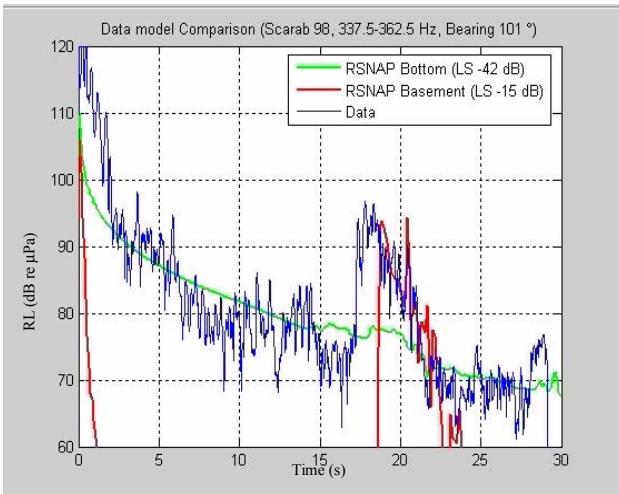


Figure 4. Comparison of data and prediction 101 true 337.5-362.5 Hz.

Using the environmental parameters shown in Table 1 and the system parameters of beamwidth and source depth, we exercised the R-SNAP model to predict the expected value of the sediment and basement reverberation for various beam angles over various bands. The results for the beam azimuth of 101 true and the 337.5-362.5 Hz frequency band are shown superimposed on the data in Fig. 4. Notice that the increase in bottom reverberation over the ridge structure for the sediment interface scattering mechanism,

shown in green, is quite slight, while the scattering from the basement is essentially non-existent until the thinning of the sediment cover over the ridge allows it to become a significant mechanism at a time of approximately 18 s. The offset between the data and the simulation is due to the use of insufficiently accurate estimates of sediment thickness.

Using the new time series simulation capability of R-SNAP, we simulated reverberation time series for the 337.5-362.5 and the 950-1050 Hz bands over the clutter-inducing Ragusa ridge. The data-model comparison for the 337.5-362.7 Hz band is shown in Fig. 5, and for the 950-1050 Hz band in Fig. 6. In each figure the data is shown in blue and the simulation in red, with 20 dB removed so as to facilitate comparison. Agreement in the lower band is quite good, including up and onto the reverberation enhancement on the ridge. In the upper band, the agreement is less good as the sediment thickness causes a significant reduction in the contribution of the basement scattering contribution. In Figs. 7 and 8 the spectrograms of the data and the model are shown side by side for the two bands. Note the time-frequency striations visible in the data are replicated in the simulations. Many of the aspects of the clutter caused by the Ragusa ridge are faithfully replicated in the simulations.

V. CONCLUSIONS

The R-SNAP code has been modified to simulate reverberation time series, and the code has been exercised to model clutter caused by an exposed ridge on the Malta Plateau. Model-data comparisons at 350 and 1000 Hz show favorable agreement between the reverberation data from the ridge and the simulations using average environmental parameters supplied by an independent analysis. These results illustrate that with sufficient environmental knowledge certain clutter characteristics of shallow water reverberation associated with large environmental features may be predicted.

REFERENCES

- [1] D. Abraham and A. Lyons, "Reverberation envelope statistics and their dependence on sonar bandwidth and scattering patch size," *IEEE J. Ocean. Eng.*, vol. 29 no. 1, pp. 126-137, January 2004.
- [2] K. D. LePage, *Monostatic reverberation in range dependent waveguides: The R-SNAP model*, SR-363, SACLANT Undersea Research Centre, La Spezia, Italy, 2003.
- [3] C. Ferla, M. Porter, and F. Jensen, *C-SNAP: Coupled SACLANTCEN normal mode propagation loss model*, SM-274, SACLANT Undersea Research Centre, La Spezia, Italy, 1993.
- [4] K.J. McCann, M. E. Ladd, and C. S. Hayek, *Upward and downward propagating mode for a normal mode treatment of reverberation*, Johns Hopkins Univ. APL Tech. Memo. No. STS-90-046, 1990.
- [5] K. D. LePage, *Modal travel time, dispersion, and approximate time series synthesis in range-dependent waveguides*, SR-350, SACLANT Undersea Research Centre, La Spezia, Italy, 2003.
- [6] W. A. Kuperman and H. Schmidt, "Self-consistent perturbation approach to rough surface scattering in stratified elastic media," *J. Acoust. Soc. Am.*, vol. 86 no. 4, pp. 1511-1522.
- [7] C. W. Holland, "Mapping seabed variability: Rapid surveying of coastal regions," *J. Acoust. Soc. Am.*, vol. 119 no. 3, pp. 1373-1387.

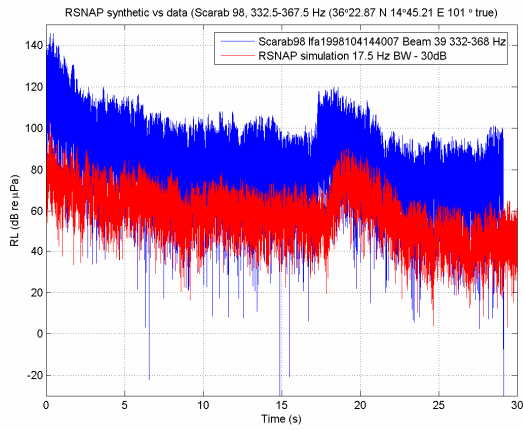


Figure 5. Data (blue)-model (red) comparison in the 337.5-362.5 Hz band

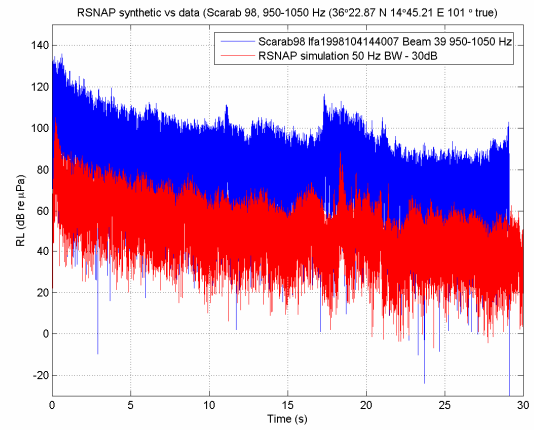


Figure 6. Data (blue)-model (red) comparison in the 950-1050 Hz band

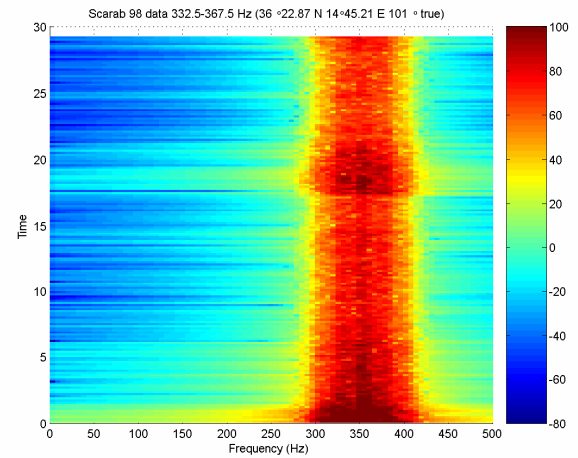
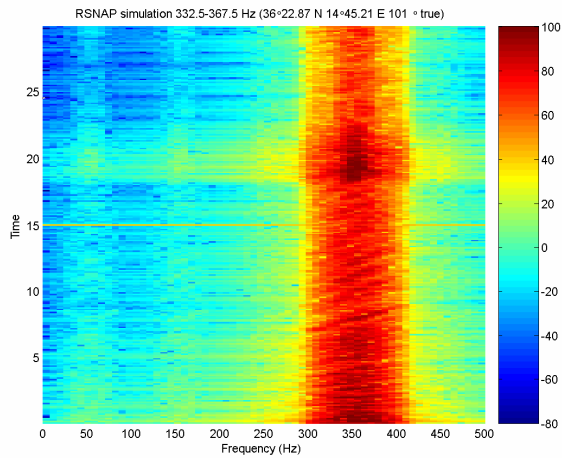


Figure 7. Spectrogram of 350 Hz simulation (left) and data (right)

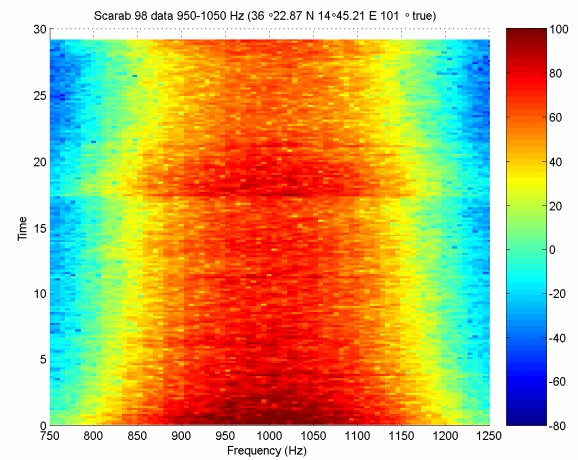
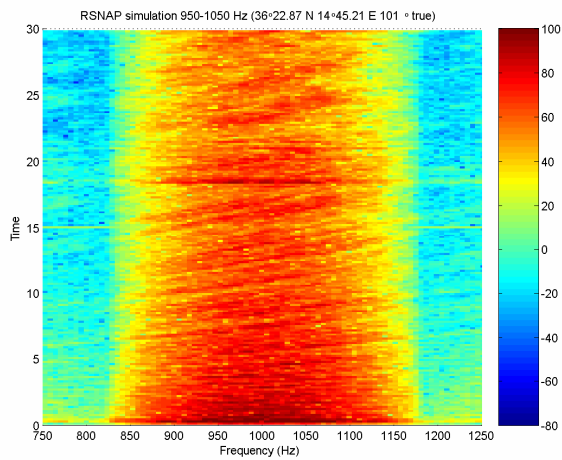


Figure 8. Spectrogram of 1kHz simulation (left) and data (right)